XUV Rectification Effect in the IR-Dressed Medium

A. V. Flegel and M. V. Frolov
Department of Physics, Voronezh State University, Voronezh 394018, Russia
and Department of Radiophysics, University of Nizhny Novgorod, Nizhny Novgorod 603950, Russia

(Received 11 January 2023; revised 26 October 2023; accepted 15 November 2023; published 11 December 2023)

We show that the quasistatic dipole moment can be induced by a short extreme ultraviolet (XUV) pulse (XUV rectification effect) in atomic gas medium subjected to an intense infrared (IR) field (IR-dressed atoms). The general theory of the XUV rectification effect for a single IR-dressed atom is presented, which explicitly relates IR-modified polarizability of an atomic system in the XUV range with the induced quasistatic dipole moment. We illustrate general properties of the XUV rectification effect in an atomic system within the analytical zero-range potential model by presenting the dependence on the IR-field intensity and the time delay between XUV and IR pulses.

DOI: 10.1103/PhysRevLett.131.243202

The optical rectification effect (ORE) is one of the well-known phenomena in nonlinear optics discovered theoretically and experimentally in the early 1960s [1–3]. This effect consists of inducing of the quasistatic dipole moment (QSDM) in a target system interacting with an intense low-frequency laser field. For a perturbative laser field, ORE can be phenomenologically described and analyzed within the second order of the perturbation theory (PT) [1], which provides an explicit expression for the second-order nonlinear susceptibility. Since the laser electric field and laser-induced dipole moment are polar vectors, the general symmetry properties with respect to the inversion reduce all even-order nonlinear susceptibilities to zero for systems having a center of inversion. From this symmetry reason, ORE cannot be observed for optically transparent systems with central symmetry (e.g., for unpolarized single atom neglecting decay effects). ORE is mainly studied for nonlinear crystals (including piezo- and ferroelectrics) [4,5], semiconductors [6–8], graphene [9], with further promising application in the development of ultrafast optical gate. For the linearly polarized laser field, the physics of this effect consists of the dichotomy of the target's response to a "positive" and "negative" directed field, e.g., caused by the presence of a preferable direction (or directions) in a target system, which breaks central symmetry. Since ORE is forbidden in the dipole approximation for centrally symmetric systems, this effect has not drawn too much attention to atomic targets. To the best of our knowledge, there was discussion of ORE in an atomic system only in Ref. [10], where it was shown that ORE can be caused by the nondipole effects in laser-atom interaction together with laser-induced dissipation channels. Since ORE is a second-order effect in the incident laser strength, the magnitude of QSDM is much less than the linear polarization response of the medium. However, ORE is well observed experimentally (see details in Refs. [2,3,6–9]), because QSDM and linear polarization response manifest in predominantly different frequency ranges: ORE is realized at the near-zero frequency range, while the linear polarization response contributes at the carrier frequency of the laser field.

In this Letter, we show that QSDM can be induced in an atomic system jointly interacting with a short extreme ultraviolet (XUV) and intense infrared (IR) laser pulses. We find that the proposed XUV rectification effect in IR-dressed atom can be realized even in the absence of any dissipation channel (e.g., XUV- or IR-induced ionization), and it can be described within the dipole approximation. If XUV-induced ionization takes place, it leads to appearance of the photoelectron alternating current with near zero frequency accompanying the XUV rectification.

Before rigorous quantum mechanical description of the XUV rectification effect for IR-dressed atom, we would like to give qualitative explanation of the physical mechanism of the proposed effect by specifying importance of shortness of the XUV pulse and IR dressing. Let us consider an atomic system jointly interacting with an intense IR and short XUV pulses. The duration of the XUV pulse ($\mathcal{T}_{\mathrm{XUV}}$) is assumed to be much smaller than the IR-field period (T_{IR}). The condition $\mathcal{T}_{\mathrm{XUV}} \ll T_{\mathrm{IR}}$ allows us to consider the IR field on the timescale $\mathcal{T}_{\mathrm{XUV}}$ as a static field with strength $\mathcal{F}_\tau = F_{\mathrm{IR}}(\tau)$ corresponding to the instantaneous IR-field strength $F_{\mathrm{IR}}(t)$ at the time-delay moment ($t = \tau$) between XUV and IR pulses. This "static" field determines a preferable direction distorting the central symmetry of a target, thereby creates a necessary condition for the XUV rectification effect on the time scale of the XUV pulse. During the time $\mathcal{T}_{\mathrm{XUV}}$, an atomic system becomes polarized through the virtual absorption and emission of the XUV photon in the presence of effective dc field $\mathcal{F}_\tau$. Obviously, the XUV-induced polarization of an atomic system leads to the dynamic Stark shift ΔE of the

bound state level in XUV and dc fields, so that the dipole moment at near-zero frequency $\mathcal{D}$ can be found as the first derivative of ΔE with respect to the strength $\mathcal{F}_\tau$ [11,12] (atomic units are used throughout this Letter unless specified otherwise):

$$\mathcal{D} = -\frac{\partial \Delta E}{\partial \mathcal{F}_\tau}, \qquad \Delta E = -\frac{F_{\mathrm{XUV}}^2}{4}\alpha(\omega_{\mathrm{XUV}}, \mathcal{F}_\tau), \quad (1)$$

where α is the dynamic polarizability of an atomic system in dc field $\mathcal{F}_\tau$, F_{XUV} and ω_{XUV} are strength and carrier frequency of the XUV pulse. Here, we assume that both fields are linearly polarized in the same direction.

In order to confirm result (1), we proceed our further analysis of the XUV rectification effect within the adiabatic approximation for IR-dressed atomic system [13,14] and the PT with respect to interaction of an atom with XUV pulse. The adiabatic treatment of IR-field-atom interaction is valid under the smallness conditions for the Keldysh parameter: $\gamma = \kappa\omega_{\mathrm{IR}}/F_{\mathrm{IR}} \ll 1$ (where $\kappa = \sqrt{2I_p}$, I_p is the ionization potential of an atomic system, F_{IR} and ω_{IR} are strength and carrier frequency of the IR field, respectively), and the frequency: $\omega_{\mathrm{IR}}/I_p \ll 1$. The PT in F_{XUV} can be used even for comparatively high intensity $\sim 10^{16}$ W/cm^2, while its validity is ensured by the smallness of the parameter $\beta_{\mathrm{XUV}} = \kappa F_{\mathrm{XUV}}/\omega_{\mathrm{XUV}}^2 < 1$ (see Refs. [15–18]).

In the frame of the adiabatic approach and the second order of the PT in F_{XUV}, the polarization response of IR-dressed atom at the near zero frequency, i.e., QSDM $d(t)$, is given by the expression [19],

$$\begin{aligned} d(t) = \frac{F_{\mathrm{XUV}}^2}{4} f_{\mathrm{XUV}}^2(t-\tau) \\ \times \Big[\langle \tilde{\Phi}_{\mathrm{dc}}|z|\Phi_{\mathrm{dc}}\rangle \langle \tilde{\Phi}_{\mathrm{dc}}|z(G_{-1}^2 + G_1^2)z'|\Phi_{\mathrm{dc}}\rangle \\ - \langle \tilde{\Phi}_{\mathrm{dc}}|z(G_{-1}z'G_{-1} + G_1 z' G_1 + G' z' G_{-1} \\ + G' z' G_1 + G_1 z' G' + G_{-1} z' G')z''|\Phi_{\mathrm{dc}}\rangle \Big], \end{aligned} \quad (2)$$

where $f_{\mathrm{XUV}}(t)$ is the envelope of the XUV pulse, Φ_{dc}, $G_{\pm 1} \equiv G_{E_0 \pm \omega_{\mathrm{XUV}}}$, and $G' \equiv G'_{E_0}$ are the wave function, Green's function, and reduced Green's function of an atomic system in the dc field $\mathcal{F}_t = F_{\mathrm{IR}}(t)$, respectively, E_0 is the energy of the IR-dressed bound state (i.e., E_0 involves the dc-induced Stark shift in the field $\mathcal{F}_t$). In Eq. (2) for the dipole moment we neglect the depletion effect of the IR-dressed bound state. This effect can be taken into account by introducing the factor $\mathcal{P}(t)$,

$$\mathcal{P}(t) = e^{-\int_0^t \Gamma(t')dt'}, \quad (3)$$

where $\Gamma(t) \equiv \Gamma(\mathcal{F}_t)$ is the total ionization rate of the IR-dressed bound state in the dc field $\mathcal{F}_t$.

The sum of matrix elements in Eq. (2) can be converted to the derivative of polarizability by utilizing the methodology of the Hellmann-Feynman theorem [19]:

$$d(t) = \frac{F_{\mathrm{XUV}}^2}{4} f_{\mathrm{XUV}}^2(t-\tau)\frac{\partial \alpha(\omega_{\mathrm{XUV}}, \mathcal{F}_t)}{\partial \mathcal{F}_t}. \quad (4)$$

For nonresonant $\omega_{\mathrm{XUV}} < |E_0|$, the atomic polarizability α is a smooth function of $\mathcal{F}_t$, while for $\omega_{\mathrm{XUV}} > |E_0|$, it rapidly oscillates as $\mathcal{F}_t$ changes. The physical origin of these oscillations has been clarified in Refs. [23,24] (see also review [11]) and connected to the two-path interference in a dc field. The first semiclassical path represents the electron motion from the dc-induced barrier, while the second path consists of electron motion toward the barrier with subsequent reflection [24]. The semiclassical phase difference between two paths is $\Delta\phi = 2(2E)^{3/2}/(3\mathcal{F}_t)$, where $E = E_0 + \omega_{\mathrm{XUV}}$ is the photoelectron energy. With decreasing $\mathcal{F}_t$, the phase difference $\Delta\phi$ increases, what leads to fast oscillations of QSDM in Eq. (4). From the mathematical point of view, the atomic Green's function $G_E(\mathcal{F})$ in dc field $\mathcal{F}$ has singular point at $\mathcal{F} = 0$, that causes the presence of analytical and nonanalytical parts in the function $G_E(\mathcal{F})$. The analytical part of Green's function has the finite derivative with respect to $\mathcal{F}$ at $\mathcal{F} = 0$ for any E, while the corresponding derivative of the nonanalytical part is zero for $E < 0$ and infinity for $E > 0$. It can be shown that only the nonanalytical part of the Green's function $G_E(\mathcal{F})$ results in the aforementioned oscillations. In the expression (4), these oscillations exceed the level of accuracy of the adiabatic approach (which assumes a smooth dependence of the IR-dressed state Φ_{dc} as $\mathcal{F}_t$ changes [14,25]). Therefore, the expression (4) for $d(t)$ should be regularized by averaging over the period of fast oscillations with respect to $\Delta\phi$. Such regularization leads to elimination of all nonanalytical dependencies of $d(t)$ on $\mathcal{F}_t$, i.e., only the analytical (smooth) part of the Green's functions should be utilized for calculation of polarizability α in Eq. (4) for QSDM. After regularization, the result for $d(t)$ involves the analytical (averaged) counterpart of the polarizability, $\bar{\alpha}(\omega_{\mathrm{XUV}}, \mathcal{F}_t)$, replacing $\alpha(\omega_{\mathrm{XUV}}, \mathcal{F}_t)$ in Eq. (4). For small $\mathcal{F}_t$, Eq. (4) provides a simple asymptotics for $d(t)$:

$$\begin{aligned} d(t) \approx \frac{F_{\mathrm{XUV}}^2}{4} f_{\mathrm{XUV}}^2(t-\tau)\mathcal{F}_t \beta(\omega_{\mathrm{XUV}}), \\ \beta(\omega_{\mathrm{XUV}}) = \lim_{\mathcal{F}\to 0}\frac{1}{\mathcal{F}}\frac{\partial \bar{\alpha}(\omega_{\mathrm{XUV}}, \mathcal{F})}{\partial \mathcal{F}}. \end{aligned} \quad (5)$$

Since the time dependence of $d(t)$ is primarily determined by the envelope of a short XUV pulse ($\mathcal{T}_{\mathrm{XUV}} \ll T_{\mathrm{IR}}$), the Fourier spectrum, $\mathcal{D}(\omega)$, of $d(t)$ weakly depends on ω in the $\omega \lesssim 1/\mathcal{T}_{\mathrm{XUV}}$ domain, i.e., there are no allocated frequencies. We calculate the static dipole moment $\mathcal{D} \equiv \mathcal{D}(\omega = 0)$ induced by XUV and IR pulses

[i.e., the zeroth harmonic of QSDM $d(t)$] by averaging $d(t)$ over the time of XUV-pulse duration $\mathcal{T}_{\rm XUV}$. Since the IR-field strength does not change sufficiently during the time $\mathcal{T}_{\rm XUV}$, the averaged QSDM can be estimated by evaluating $d(t)$ in Eq. (4) at the instant $t=\tau$ and multiplying it by a factor $\mathcal{S}$ depending on the shape of the XUV pulse:

$$\mathcal{D}=\frac{1}{\mathcal{T}_{\rm XUV}}\int_{-\infty}^{\infty}d(t)dt\approx\frac{F_{\rm XUV}^2}{4}\frac{\partial\bar{\alpha}(\omega_{\rm XUV},\mathcal{F}_\tau)}{\partial\mathcal{F}_\tau}\mathcal{S},$$
$$\mathcal{S}=\frac{1}{\mathcal{T}_{\rm XUV}}\int_{-\infty}^{\infty}f_{\rm XUV}^2(t)dt. \quad (6)$$

Our rigorous quantum mechanical result (6) for the averaged QSDM $\mathcal{D}$ differs from the qualitative expression (1) by the pulse-shape factor $\mathcal{S}$ (which is close to unity for most shapes) and the averaged dynamic polarizability $\bar{\alpha}$.

We emphasize that for $\omega_{\rm XUV}>|E_0|$ the atomic polarizability has the imaginary part indicating a dissipative process through the one-photon ionization (the contribution of the tunneling ionization channel induced by the IR field is negligible for the moderate IR-field intensities considered in this work). In order to interpret the physical meaning of real and imaginary parts of QSDM, keep in mind the meaning of real and imaginary parts of polarizability α. The real part of α contributes to the Stark shift of an atomic level, and thereby determines the polarization of an atomic target at the XUV frequency, while the imaginary part of α gives the one-photon ionization rate or the total laser-induced photoelectric current. Similarly, the real and imaginary parts of complex QSDM represent, respectively, the polarization of an atomic target and the total current at the near zero frequencies.

The analytic form of the dc-field-distorted dynamic polarizability $\alpha(\omega_{\rm XUV},\mathcal{F})$ for arbitrary $\mathcal{F}$ is unknown for any neutral atom, and its calculation is on the same footing of complexity as the numerical integration of the time-dependent Schrödinger equation. For this reason, we proceed our analysis within the zero-range potential model [26], for which the analytic expression of $\alpha(\omega_{\rm XUV},\mathcal{F})$ is known and presented in terms of a product of Airy functions [11]. For regularization $\alpha(\omega_{\rm XUV},\mathcal{F}_t)$, i.e., for averaging it over the fast oscillations with respect to $\Delta\phi\gg1$, we use the representation of Airy functions in terms of modulus and phase. Since the phase of the involved Airy functions is well approximated by $\Delta\phi$ [27], the regularization procedure consists of the averaging of products of Airy functions with respect to their phases [19].

For our modeling calculation we consider an artificial atomic system with the ionization potential $I_p=15.76$ eV. The IR field is considered as the 3-cycle pulse with $\sin^2$ envelope having carrier frequency $\omega_{\rm IR}=0.0285$ a.u. ($\hbar\omega_{\rm IR}=0.775$ eV, and $\lambda_{\rm IR}=1.6$ μm), the pulse duration $\mathcal{T}_{\rm IR}=16$ fs (i.e., FWHM is 8 fs), and the peak intensity in the range $I_{\rm IR}=cF_{\rm IR}^2/(8\pi)=0.05-0.5$ PW/cm^2 (c is the speed of light):

$$F_{\rm IR}(t)=F_{\rm IR}f_{\rm IR}(t)\cos(\omega_{\rm IR}t),$$
$$f_{\rm IR}(t)=\begin{cases}\sin^2(\pi t/\mathcal{T}_{\rm IR}), & \text{for } t\in[0,\mathcal{T}_{\rm IR}],\\ 0, & \text{otherwise.}\end{cases}$$

It is worth noting, that for intensities used in our calculations, the model-based estimation of the depletion factor $\mathcal{P}(t)$ in Eq. (3) gives $\mathcal{P}(t)\gtrsim0.98$, so that the depletion effects of initial state should not lead to any noticeable distortion of our further results. [The magnitude of $\mathcal{P}(t)$ depends on multielectron effects in an IR-perturbed atomic system and can differ significantly from the single-active electron model (see, e.g., Ref. [28]).] The XUV pulse with Gaussian shape is parametrized as

$$F_{\rm XUV}(t)=F_{\rm XUV}e^{-(2\ln2)t^2/\mathcal{T}_{\rm XUV}^2}\cos(\omega_{\rm XUV}t),$$

where the carrier frequency $\omega_{\rm XUV}=2.205$ a.u. ($\hbar\omega_{\rm XUV}=60$ eV), the pulse duration $\mathcal{T}_{\rm XUV}=600$ as ($\mathcal{T}_{\rm XUV}=0.1\mathcal{T}_{\rm IR}$), and the peak intensity $I_{\rm XUV}=cF_{\rm XUV}^2/(8\pi)=0.1$ PW/cm^2.

In Fig. 1 we present the dependence of averaged QSDM $\mathcal{D}$ on the time delay τ [29]. For small and moderate intensities (up to $I_{\rm IR}=0.1$ PW/cm^2), the time delay dependence of both real and imaginary parts of $\mathcal{D}$ perfectly replicates the waveform of the IR pulse. For this range of intensity, the average QSDM can be approximated by the linear dependence on $F_{\rm IR}(\tau)$, that agrees with approximation (5) for $d(t)$. For higher intensities (see line for $I_{\rm IR}=0.5$ PW/cm^2 in Fig. 1), noticeable deviations from the

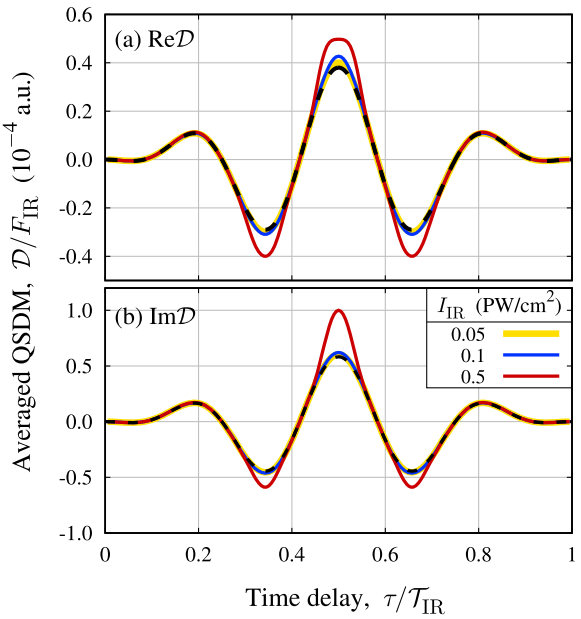

FIG. 1. The ratio of real (a) and imaginary (b) parts of averaged QSDM to the peak IR-field strength ($\mathcal{D}/F_{\rm IR}$) as functions of the time delay τ between XUV and IR pulses for different IR-pulse intensities $I_{\rm IR}$ shown in the figure legend. Dashed black lines show the scaled profile of $-F_{\rm IR}(\tau)$.

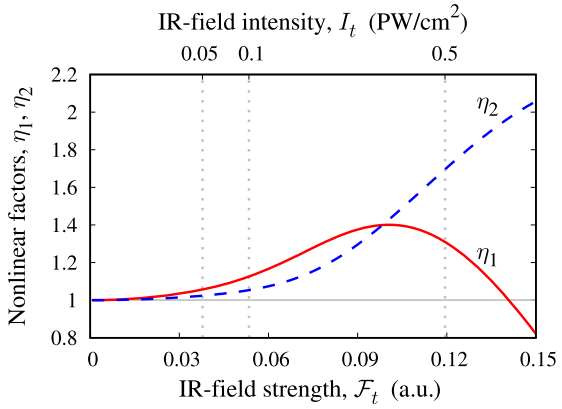

FIG. 2. The dependence of nonlinear factors η_1 (solid red line) and η_2 (dashed blue line) [see Eq. (7)] on the instantaneous IR-field strength $\mathcal{F}_t$ and instantaneous intensity I_t. Vertical dotted lines indicate values of $\mathcal{F}_t$ and I_t corresponding to the IR-pulse peak intensities in Fig. 1.

linear dependence $\mathcal{D} \propto F_{\rm IR}(\tau)$ appear in the regions of local extrema of the function $F_{\rm IR}(\tau)$ lying near the center of the IR pulse. In order to specify the contribution of nonlinear effects in $\bar{\alpha}$ with respect to the IR-field strength, we introduce the nonlinear factors η_1 and η_2:

$$\eta_1 = \frac{1}{\mathcal{F}_t \mathrm{Re}\beta}\frac{\partial \mathrm{Re}\bar{\alpha}}{\partial \mathcal{F}_t}, \qquad \eta_2 = \frac{1}{\mathcal{F}_t \mathrm{Im}\beta}\frac{\partial \mathrm{Im}\bar{\alpha}}{\partial \mathcal{F}_t}. \tag{7}$$

If nonlinear effects are small, factors η_1 and η_2 are close to unity. The dependence of η_1 and η_2 on the instantaneous IR-field strength $\mathcal{F}_t$ and corresponding IR-field intensity $I_t = c\mathcal{F}_t^2/(8\pi)$ is shown in Fig. 2. As is seen from the figure, the contribution of nonlinear effects appears for $\mathcal{F}_t \gtrsim 0.05$ a.u. ($I_t \gtrsim 0.1$ PW/cm^2). Note that for high intensities ($I \gtrsim 0.5$ PW/cm^2), along the nonlinear effects, the IR-induced depletion of a target can have a significant impact on the XUV rectification.

In Fig. 3 we present a color-coded map for the dependence of the real part of QSDM, Red, on the time t and time delay τ between IR and XUV pulses [the result is obtained within Eq. (4), where α is replaced by $\bar{\alpha}$]. We do not present the imaginary part of QSDM, since as it follows from approximation (5) (which is appropriate for the used IR-field intensity, $I_{\rm IR} = 0.1$ PW/cm^2), Imd/Im$\beta \approx$ Red/Reβ, and both real and imaginary parts of d have similar behavior. Our calculations show that the distribution of $d(t;\tau)$ is localized around the line $t = \tau$ forming the stripe with effective width $\mathcal{T}_{\rm XUV}/\sqrt{2}$. For fixed τ, the temporal profile of QSDM is presented by a narrow burst (see violet lines in Fig. 3) with full width at half maximum equal to $\mathcal{T}_{\rm XUV}$. The shape of these bursts for most τ replicates the profile of the squared XUV-pulse envelope $f^2_{\rm XUV}(t)$. However, for a time delay near zero t_0 of the IR field [i.e., for $|\tau - t_0| \lesssim \mathcal{T}_{\rm XUV}$, where $F_{\rm IR}(t_0) = 0$], the t dependence of QSDM becomes asymmetric with respect to the

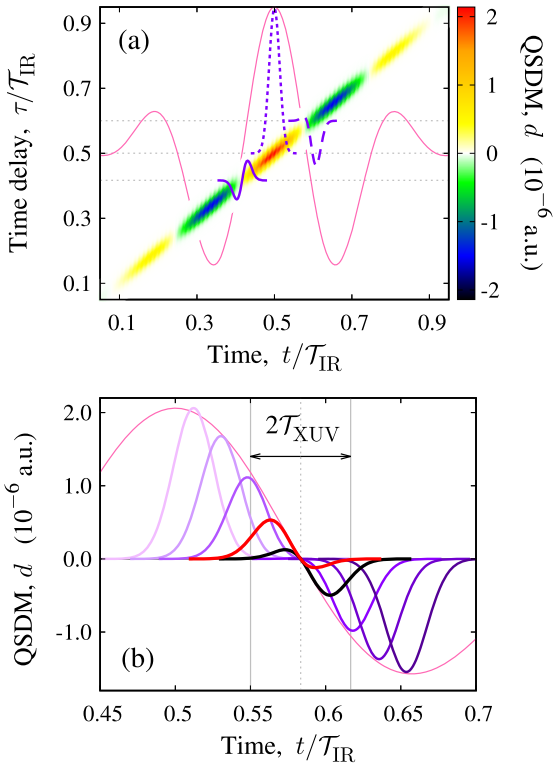

FIG. 3. (a) Color-coded map for the time evolution of the real part of QSDM, Re$d(t)$, as a function of the time delay τ. Thick violet lines show the temporal profiles of Re$d(t)$ (in arbitrary units) for fixed values of τ: $0.417\mathcal{T}_{\rm IR}$—solid line; $0.5\mathcal{T}_{\rm IR}$—dotted line; $0.6\mathcal{T}_{\rm IR}$—dashed line. (b) Re$d(t)$ for different τ: each solid line from left to right corresponds to the value of $\tau/\mathcal{T}_{\rm IR}$ from 0.513 to 0.653 with increment of 0.02. Vertical dashed gray line indicates the position of IR-field zero $t_0 = 0.583\mathcal{T}_{\rm IR}$, vertical solid gray lines indicate points $t_0 \pm \mathcal{T}_{\rm XUV}$. Thin solid pink lines in both panels show the scaled temporal profile of $-F_{\rm IR}(t)$. The laser parameters are the same as in Fig. 1, $I_{\rm IR} = 10^{14}$ W/cm^2.

time $t = \tau$ [see red and black lines in Fig. 3(b)]. For $\tau = t_0$, $d(t)$ represents odd (sin-like) dependence [see violet line for $\tau = 0.417\mathcal{T}_{\rm IR}$ in Fig. 3(a)].

In conclusion, we have theoretically shown that the XUV rectification effect can be observed for a single IR-dressed atom. Our approach is based on the second-order PT (in the XUV field) for an atomic system, whose IR-laser-induced dynamics is considered within the adiabatic approximation. Our theoretical analysis shows that the atomic QSDM $d(t)$ can be induced on the attosecond timescale determined by the XUV pulse duration. The direction of $d(t)$ is given by the opposite direction of IR-field strength $F_{\rm IR}(\tau)$ at the instant corresponding to the time delay τ between IR and XUV pulses. The short duration of QSDM and its IR-controllable direction make it possible to use the XUV rectification for ultrafast optical gating. The detection of the XUV rectification effect requires in fact the measurement of a weak static electric field (determined by the static polarization), which can be realized through the application

of the E-field sensor technology [30]. Assuming that the time delay between two pulses is well stabilized, the measurement of the laser-induced QSDM using the E-field sensing implements the optical gating.

The XUV rectification effect is illustrated within the zero-range potential model. Despite the known limitations of this model, it allowed us to identify the main qualitative features of the considered effect. In particular, along with the indicated properties of the time dependence of QSDM, we have presented the range of IR-field intensities for which IR-induced nonlinear effects become significant, thereby illuminating the limits of linear approximation for the XUV rectification effect with respect to the IR-field strength. It should be noted that XUV-induced inner collective electron dynamics is implemented on the attosecond timescale [31–33] and can significantly change the magnitude of QSDM up to its elimination. For this reason, the considered XUV pulse durations should be much longer than relaxation or excitation times of a target, because it ensures the system integrity for the XUV-interaction time. An analysis of the collective electron dynamics effects deserves separate consideration.

This work was supported by Russian Science Foundation (theory development, 22-12-00223), Ministry of Science and Higher Education of the Russian Federation (zero-range potential simulations, 075-15-2021-1351).

[1] J. A. Armstrong, N. Bloembergen, J. Ducuing, and P. S. Pershan, Interactions between light waves in a nonlinear dielectric, Phys. Rep. **127**, 1918 (1962).
[2] M. Bass, P. A. Franken, J. F. Ward, and G. Weinreich, Optical rectification, Phys. Rev. Lett. **9**, 446 (1962).
[3] M. Bass, P. A. Franken, and J. F. Ward, Optical rectification, Phys. Rep. **138**, A534 (1965).
[4] L. D. Landau and E. M. Lifshitz, *Electrodynamics of Continuous Media* (Pergamon Press, Oxford, 1984).
[5] B. N. Morozov and Yu. M. Aĭvazyan, Optical rectification effect and its applications (review), Quantum Electron. **10**, 1 (1980).
[6] X.-C. Zhang, Y. Jin, K. Yang, and L. J. Schowalter, Resonant nonlinear susceptibility near the GaAs band gap, Phys. Rev. Lett. **69**, 2303 (1992).
[7] D. Côté, N. Laman, and H. M. van Driel, Rectification and shift currents in GaAs, Appl. Phys. Lett. **80**, 905 (2002).
[8] C. Van Vlack and S. Hughes, Carrier-envelope-offset phase control of ultrafast optical rectification in resonantly excited semiconductors, Phys. Rev. Lett. **98**, 167404 (2007).
[9] M. M. Glazov and S. D. Ganichev, High frequency electric field induced nonlinear effects in graphene, Phys. Rep. **535**, 101 (2014).
[10] N. L. Manakov and A. G. Fainshtein, Nonlinear-optics phenomena due to dissipative or nonstationary processes, Zh. Eksp. Teor. Fiz. **87**, 1552 (1984) [Sov. Phys. JETP **60**, 890 (1984)].
[11] N. L. Manakov, M. V. Frolov, A. F. Starace, and I. I. Fabrikant, Interaction of laser radiation with a negative ion in the presence of a strong static electric field, J. Phys. B **33**, R141 (2000).
[12] M. V. Frolov, A. V. Flegel, N. L. Manakov, and A. F. Starace, Description of harmonic generation in terms of the complex quasienergy. I. General formulation, Phys. Rev. A **75**, 063407 (2007).
[13] O. I. Tolstikhin and T. Morishita, Adiabatic theory of ionization by intense laser pulses: Finite-range potentials, Phys. Rev. A **86**, 043417 (2012).
[14] A. V. Flegel, N. L. Manakov, Ia. V. Breev, and M. V. Frolov, Adiabatic expressions for the wave function of an electron in a finite-range potential and an intense low-frequency laser pulse, Phys. Rev. A **104**, 033109 (2021).
[15] N. L. Manakov and A. G. Fainshtein, Quasistationary quasienergy states and convergence of perturbation series in a monochromatic field, Theor. Math. Phys. **48**, 815 (1981).
[16] N. L. Manakov, M. V. Frolov, B. Borca, and A. F. Starace, Multiphoton detachment of a negative ion by an elliptically polarized, monochromatic laser field, J. Phys. B **36**, R49 (2003).
[17] E. A. Pronin, A. F. Starace, M. V. Frolov, and N. L. Manakov, Perturbation theory analysis of attosecond photoionization, Phys. Rev. A **80**, 063403 (2009).
[18] L.-Y. Peng, E. A. Pronin, and A. F. Starace, Attosecond pulse carrier-envelope phase effects on ionized electron momentum and energy distributions: Roles of frequency, intensity and an additional IR pulse, New J. Phys. **10**, 025030 (2008).
[19] See Supplemental Material at http://link.aps.org/supplemental/10.1103/PhysRevLett.131.243202 for derivation details of the base expression for QSDM and expressions for the atomic dynamic polarizability within the zero-range potential model, which includes additional Refs. [20–22].
[20] R. M. More and E. Gerjuoy, Properties of resonance wave functions, Phys. Rev. A **7**, 1288 (1973).
[21] D. K. Watson, Partial widths and resonance normalization, Phys. Rev. A **34**, 1016 (1986).
[22] P. W. Langhoff, S. T. Epstein, and M. Karplus, Aspects of time-dependent perturbation theory, Rev. Mod. Phys. **44**, 602 (1972).
[23] V. D. Kondratovich and V. N. Ostrovskil, Photoionization of a hydrogenlike atom in a homogeneous electric field, Zh. Eksp. Teor. Fiz. **79**, 395 (1980) [Sov. Phys. JETP **52**, 198 (1980)].
[24] I. I. Fabrikant, Interference effects in photodetachment and photoionization of atoms in a homogeneous electric field, Zh. Eksp. Teor. Fiz. **79**, 2070 (1980) [Sov. Phys. JETP **52**, 1045 (1980)].
[25] A. A. Romanov, A. A. Silaev, N. V. Vvedenskii, Ia. V. Breev, A. V. Flegel, and M. V. Frolov, Second-harmonic generation of a short XUV pulse interacting with an IR-laser-dressed atom, Phys. Rev. A **106**, 063101 (2022).
[26] Yu. N. Demkov and V. N. Ostrovsky, *Zero-Range Potentials and Their Applications in Atomic Physics* (Plenum, New York, 1988).
[27] *NIST Digital Library of Mathematical Functions*, https://dlmf.nist.gov/, Release 1.1.11 of 2023-09-15, edited by

F. W. J. Olver, A. B. Olde Daalhuis, D. W. Lozier, B. I. Schneider, R. F. Boisvert, C. W. Clark, B. R. Miller, B. V. Saunders, H. S. Cohl, and M. A. McClain.

[28] A. A. Romanov, A. A. Silaev, M. V. Frolov, and N. V. Vvedenskii, Influence of the polarization of a multi-electron atom in a strong laser field on high-order harmonic generation, Phys. Rev. A **101**, 013435 (2020).

[29] The time delay between IR and XUV pulses is introduced as follows: for $\tau < \mathcal{T}_{\mathrm{IR}}/2$ the XUV pulse is ahead of the IR one, while for $\tau > \mathcal{T}_{\mathrm{IR}}/2$ vice versa. The total field of two pulses at time t is $F_{\mathrm{IR}}(t) + F_{\mathrm{XUV}}(t-\tau)$.

[30] I. Shoji, H. Wada, K. Uto, Y. Takeda, T. Sugimoto, and H. Matsui, Visualizing quasi-static electric fields with flexible and printed organic transistors, Adv. Mater. Tech. **6**, 2100723 (2021).

[31] M. Uiberacker, Th. Uphues, M. Schultze, A. J. Verhoef, V. Yakovlev, M. F. Kling, J. Rauschenberger, N. M. Kabachnik, H. Schröder, M. Lezius, K. L. Kompa, H. G. Muller, M. J. J. Vrakking, S. Hendel, U. Kleineberg, U. Heinzmann, M. Drescher, and F. Krausz, Attosecond real-time observation of electron tunnelling in atoms, Nature (London) **446**, 627 (2007).

[32] R. Pazourek, J. Feist, S. Nagele, and J. Burgdörfer, Attosecond streaking of correlated two-electron transitions in helium, Phys. Rev. Lett. **108**, 163001 (2012).

[33] M. Ossiander, F. Siegrist, V. Shirvanyan, R. Pazourek, A. Sommer, T. Latka, A. Guggenmos, S. Nagele, J. Feist, J. Burgdörfer, R. Kienberger, and M. Schultze, Attosecond correlation dynamics, Nat. Phys. **13**, 280 (2016).